Available online at www.sciencedirect.com
ScienceDirect
Polymer 47 (2006) 8297–8308
polymer
www.elsevier.com/locate/polymer

Synthesis of laterally attached side-chain liquid crystalline poly(*p*-phenylene vinylene) and polyfluorene derivatives for the application of polarized electroluminescence

Yung-Hsin Yao, Sheng-Hsiung Yang, Chain-Shu Hsu*

Department of Applied Chemistry, National Chiao Tung University, 1001 Ta-Hsueh Road, Hsinchu 30010, Taiwan, ROC

Received 16 August 2006; received in revised form 5 October 2006; accepted 6 October 2006
Available online 27 October 2006

Abstract

Two series of poly(*p*-phenylene vinylene) and polyfluorene derivatives (**PPV1**–**PPV4** and **PF1**–**PF5**) containing laterally attached penta(*p*-phenylene) mesogenes were synthesized and characterized. These polymers show nematic liquid crystalline behavior. The optical properties of the polymers were investigated by UV–vis absorption and photoluminescence spectrometers and these polymers were fabricated to form the polarized electroluminescent devices using poly(ethylenedioxythiophene)–poly(styrene sulfonic acid) (PEDOT–PSS) as an alignment layer. In the series of poly(*p*-phenylene vinylene) derivatives, polymer **PPV4** offered the best EL device performance. It emitted yellow light at 588 nm at 4 V. The maximum brightness was about 1337 cd/m^2 at 9 V with a polarized ratio of 2.6. In another series of polyfluorene derivatives, **PF4** offered the best EL device performance with the polarized ratio of 12.4 and a maximum luminescence of 1855 cd/m^2. In the case of polarized white light, as a consequence of blending small amount of **PF4** and **PF5** with a host polymer **PF2**, polarized ratio of up to 10.2 and a maximum brightness of 2454 cd/m^2 have been attained. The aligned films exhibited pronounced polarized ratio, implying that the polymers exhibit potential for linearly polarized LED application.

Keywords: Poly(*p*-phenylene vinylene); Polyfluorene; Polarized light

1. Introduction

Since the first report on polymer light-emitting diodes (PLED) [1], a number of π-conjugated polymers have been intensively investigated in order to fabricate devices for industrial applications [2–4]. Among them, poly(1,4-phenylene vinylene) (PPV) and polyfluorene (PF) as well as their derivatives show great promise for PLED applications [5].

In 1995, Inganas et al. demonstrated a PLED device based on aligned conjugated polymers which directly emitted polarized light and realized that such devices would be particularly useful as backlights for conventional liquid crystal displays (LCDs) [6]. This will simplify LCD manufacturing and reduce cost. In principle, the liquid crystalline oligomers and conjugated polymers which can be aligned under a mesomorphic phase to achieve monodomain thin film, are the best candidates for the manufacturing of highly polarized electroluminescence (EL) devices [7–21]. Among them, oligo(fluorene)s show very promising properties in polarized emission. Chen et al. synthesized some oligo(fluorene)s with different chain lengths and chromophores [17,18]. These materials show liquid crystalline behavior and polarized white light emission can be obtained by blending method. It showed a polarization ratio of 16 and a luminance yield of 4.5 cd/A; however, no brightness data were reported in that work. Besides, the preparation of these state-of-art materials strongly depends on synthetic skills. Relatively, PFs made by well-known Suzuki-coupling polymerization are easier to obtain. With proper side chains, PFs can also exhibit liquid crystallinity and be used for the fabrication of polarized EL devices. Very recently Wen et al. demonstrated blue-light polarized PLED using aligned polyfluorene [19]. The best device showed a high dichroic ratio of 25.7 (at 451 nm emission wavelength), while the brightness approached 1000 cd/m^2 at a low

* Corresponding author. Tel./fax: +886 3 5131523.
E-mail address: cshsu@mail.nctu.edu.tw (C.-S. Hsu).

0032-3861/$ - see front matter © 2006 Elsevier Ltd. All rights reserved.
doi:10.1016/j.polymer.2006.10.002

biased voltage. An additional rubbed PVK layer was used to align PF. Our group has also demonstrated polarized white emission from blending three PF derivatives [20], yet the EL dichroic ratio was not very high (up to 4.6). It seems that the liquid crystallinity of common PF polymers is less sufficient to align thin films. A further modification by incorporating laterally attached liquid crystalline moieties on the main chain to improve dichroic ratio is thus proposed and executed in this work.

In 2000 our laboratory reported poly(2,3-diphenyl-1,4-phenylene vinylene) derivatives having liquid crystalline side groups [21]. These polymers exhibit a nematic phase and have potential application for polarized electroluminescence. When these polymers were rubbed at a liquid crystalline state, the mesogenic side groups were aligned along the rubbing direction and the conjugated polymer backbones were forced to align more or less perpendicular to the rubbing direction (Fig. 1). Nevertheless, under such situation, the alignment of polymer backbones was very poor since the polymer backbones were not involving in the formation of mesophases and the polarized ratio of EL emission was very low (up to 2.1). To solve this problem, the best strategy is to synthesize conjugated polymer with laterally attached mesogens. It is well-documented that the side-chain liquid crystalline polymers with the laterally attached mesogens have tendency to form a nematic phase [22–26]. The large extended mesogens force a polymer backbone to take extended conformation due to the mesogen-jacket surrounding it.

In this paper, we synthesized two series of PPV and PF derivatives containing laterally attached penta(*p*-phenylene) mesogens. To our best knowledge, this is the first example of such kinds of liquid crystalline conjugated polymers with laterally attached mesogens. The mesomorphic behaviors as well as polarized PL and EL properties of these polymers were studied.

2. Experimental section

2.1. Materials

4-Butyl-4′-iodobiphenyl, 4-methoxyphenyl, 1,8-bromooctane, *n*-butyl lithium, 2-isopropoxy-4,4,5,5-tetramethyl-1,3,2-dioxaborolane and the other reagents were purchased from Aldrich and used as received. Tetrahydrofuran (THF) and dichloromethane were distilled and dried from sodium/benzophenone and calcium hydride, respectively. Monomers 1,4-bis(bromomethyl)-2-methoxy-5-octyloxybenzene (**M3**), 2,7-bis(4,4,5,5-tetramethyl-1,3,2-dioxaborolan-2-yl)-9,9-dioctylfluorene (**M4**), 2,7-dibromo-9,9-dioctylfluorene (**M5**), 4,7-dibromo-2,1,3-benzothiadiazole (**M6**) and 4,7-bis(5-bromo-2-thienyl)-2,1,3-benzothiadiazole (**M7**) and the end capping agents (1-bromo-4-(*tert*-butyl) benzene and 1-(*tert*-butyl)-4-(4,4,5,5-tetramethyl-1,3,2-dioxaborolan-2-yl) benzene) used in the Suzuki coupling for polyfluorenes, were prepared according to the previously published procedures [27–30].

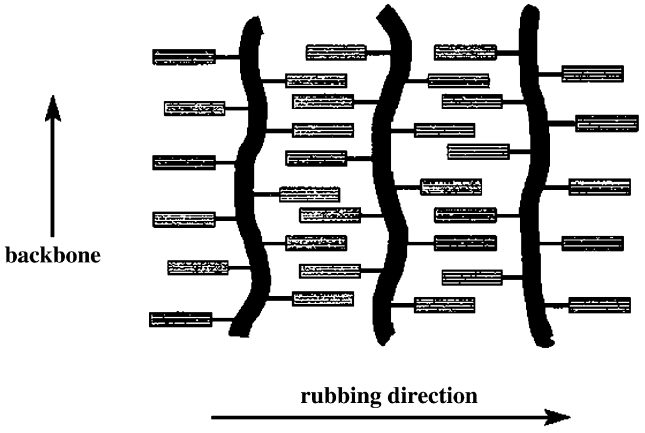

Fig. 1. Alignment of LC side groups and polymer backbones due to rubbing treatment.

2.2. Characterizations

^{1}H and ^{13}C NMR spectra were recorded on a Varian 300 spectrometer using tetramethylsilane as internal references. Gel permeation chromatography (GPC) was obtained through a VE-2001 GPC in THF using a calibration curve of polystyrene standards. Thermal transitions of monomers and polymers were determined on a Perkin–Elmer Pyris 1 differential scanning calorimeter (DSC) with a heating/cooling rate of 10 °C/min. A Carl-Zeiss Axiphot polarized optical microscope (POM) equipped with a Mettler FP82 hot stage and an FP80 central processor were used to analyze the anisotropic textures. The polarized ultraviolet–visible (UV–vis) spectra were measured on a Shimadzu UV-1601 spectrophotometer with a polarizer placed between sample and detector. Spectra were measured with the polarizer aligned parallel and perpendicular to the rubbing direction. Polarized ratios were defined as the parallel to perpendicular intensity. Polarized photoluminescence (PL) and electroluminescence (EL) were measured, respectively, on a Shimadzu RF-5301 PC spectrofluoro-photometer and a Photo Research PR-650 spectrophotometer with a polarizer placed between sample and detector.

2.3. Synthesis of monomers *M1* and *M2*, and model compound *LC1*

Scheme 1 outlines the synthetic routes for monomers **M1** and **M2**, and model compound **LC1**.

2.3.1. 2-(4′-Butyl-biphenyl-4-yl)-4,4,5,5-tetramethyl-[1,3,2]dioxaborolane (*1*)

To a solution of 4-butyl-4′-iodobiphenyl (5.0 g, 14.9 mmol) in THF (50 mL) at −78 °C, 10.2 mL of *n*-butyl lithium (16.4 mmol, 1.6 M in hexane) was added. The mixture was stirred at −78 °C for 1 h and then 2-isopropoxy-4,4,5,5-tetramethyl-1,3,2-dioxaborolane (3.3 mL, 16.4 mmol) was added slowly to the solution. The resulting mixture was warmed to room temperature and stirred at room temperature for 12 h and then 50 mL of ethyl acetate was added. The resulting solution was washed with brine and dried over magnesium sulfate. The crude product isolated by evaporating the solvent

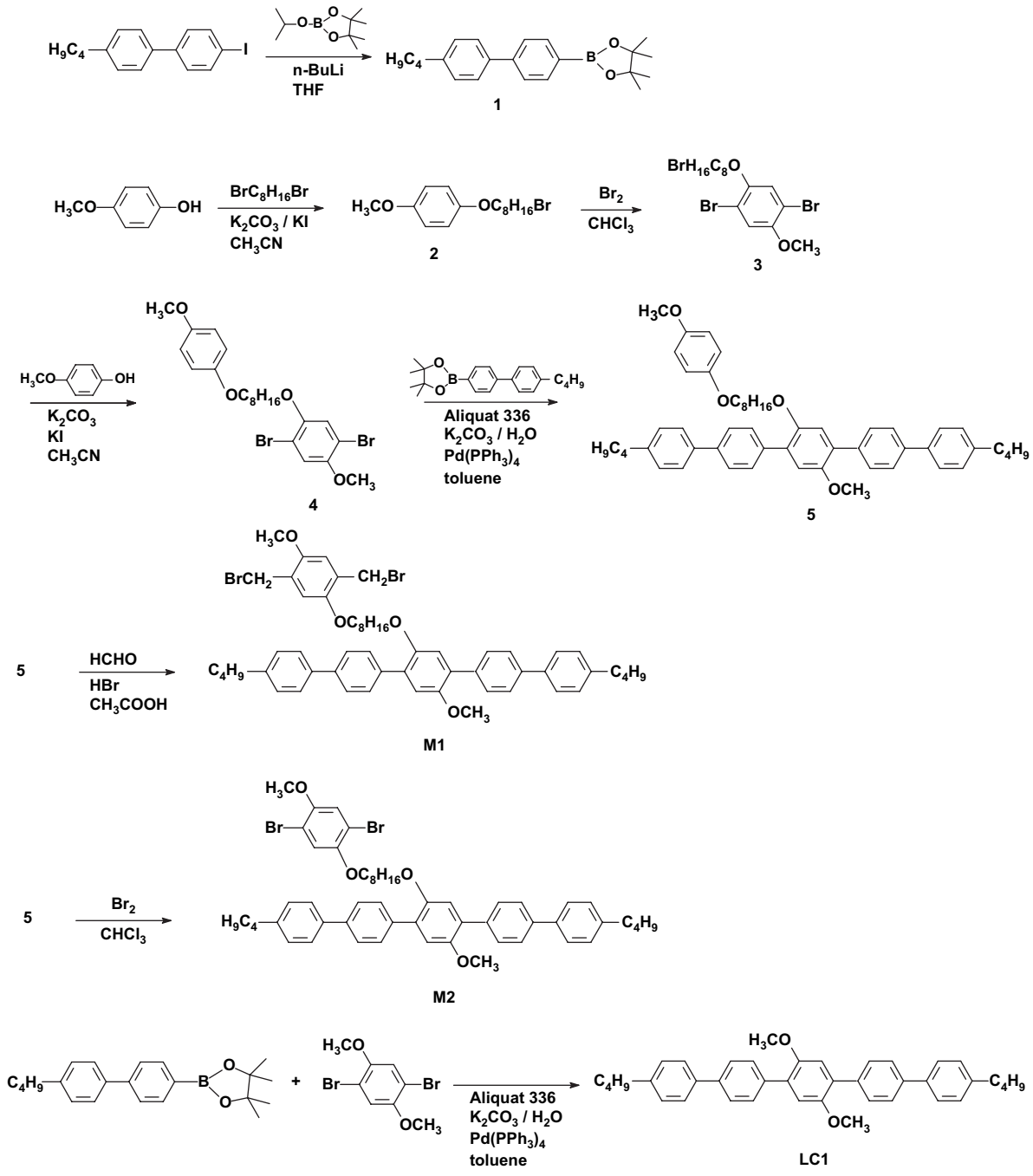

Scheme 1. Synthesis of monomers (**M1** and **M2**) and **LC1**.

and was purified by recrystallization from hexane to yield 2.55 g (51%) of white crystals; mp 76–77 °C. MS (EI, *m/z*): 336 (M^+). ^{1}H NMR ($CDCl_3$, δ ppm): 0.95 (t, $J = 7.5$ Hz, 3H, $-C_3H_6-CH_3$), 1.39 (m, 2H, $-CH_2-CH_3$), 1.40 (s, 12H, $-B-O-C(CH_3)_2-C(CH_3)_2-O-$), 1.58–1.66 (m, 2H, $-CH_2-CH_2-CH_2-CH_3$), 2.66 (t, $J = 7.5$ Hz, 2H, $-CH_2-C_3H_7$), 7.26 (d, $J = 9.0$ Hz, 2H, aromatic-H), 7.54 (d, $J = 9.0$ Hz, 2H, aromatic-H), 7.61 (d, $J = 9.0$ Hz, 2H, aromatic-H), 7.88 (d, $J = 9.0$ Hz, 2H, aromatic-H). ^{13}C NMR ($CDCl_3$, δ ppm): 13.6, 22.4, 24.6, 33.9, 35.5, 83.6, 107.4, 127.1, 128.3, 129.2, 138.3, 139.4, 142.4, 146.5, 167.9.

2.3.2. 1-(8-Bromoctyloxyl)-4-methoxybenzene (2)

4-Methoxyphenol (5.0 g, 40.3 mmol), 1,8-dibromooctane (21.9 g, 80.5 mmol), potassium carbonate (11.1 g, 80.5 mmol), and potassium iodide (1.34 g, 8.05 mmol) were dissolved in 200 mL of acetonitrile under nitrogen atmosphere. The mixture was heated to 80 °C for 24 h. Excess potassium carbonate was filtered off. The solvent was evaporated and the solid was dissolved in ethyl acetate. The ethyl acetate solution was extracted with 5% hydrochloric acid and then washed with water, saturated NaCl solution and dried over anhydrous $MgSO_4$. After evaporating the solvent, the crude product was purified by silica

gel column chromatography using ethyl acetate/hexane (1:4 by volume) as eluent to yield 11.8 g (93%) of white crystals; mp 85–86 °C. MS (EI, *m/z*): 315 (M^+). ^{1}H NMR ($CDCl_3$, δ ppm): 1.34–1.44 (m, 8H, $-OCH_2CH_2-(CH_2)_4-$), 1.73–1.88 (m, 4H, $-OCH_2CH_2-(CH_2)_4-CH_2CH_2Br$), 3.41 (t, $J = 6.0$ Hz, 2H, $-CH_2Br$), 3.77 (s, 3H, $-OCH_3$), 3.90 (t, $J = 7.5$ Hz, 2H, $-OCH_2-$), 6.83 (s, 4H, aromatic-H). ^{13}C NMR ($CDCl_3$, δ ppm): 25.2, 27.2, 27.9, 28.3, 28.8, 33.1, 33.3, 55.6, 68.3, 114.5, 116.3, 154.7, 156.8.

2.3.3. 1,4-Dibromo-2-(8-bromoctyloxy)-5-methoxybenzene (*3*)

Bromine (1.47 mL, 28.5 mmol) was added dropwise to a chloroform (50 mL) solution of **1** (3.0 g, 9.5 mmol). The reaction mixture was stirred at room temperature for 12 h, and excess bromine was quenched with sodium thiosulphate aqueous solution. The organic layers were collected, washed with water, and then dried over anhydrous magnesium sulfate. After organic solvent was evaporated, 4.13 g of yellowish liquid was obtained; yield 92%. MS (EI, *m/z*): 473 (M^+). ^{1}H NMR ($CDCl_3$, δ ppm): 1.37–1.47 (m, 8H, $-OCH_2CH_2-(CH_2)_4-$), 1.78–1.88 (m, 4H, $-OCH_2CH_2-(CH_2)_4-CH_2CH_2Br$), 3.41 (t, $J = 6.0$ Hz, 2H, $-CH_2Br$), 3.77 (s, 3H, $-OCH_3$), 3.90 (t, 2H, $J = 7.5$ Hz, 2H, $-OCH_2-$), 7.10 (s, 2H, aromatic-H). ^{13}C NMR ($CDCl_3$, δ ppm): 25.6, 27.3, 28.0, 28.8, 33.0, 33.2, 56.6, 67.2, 115.1, 115.3, 153.7, 154.2.

2.3.4. 1,4-Dibromo-2-methoxy-5-[8-(4-methoxyphenoxy)-octan-1-yloxy]benzene (*4*)

4-Methoxyphenol (0.44 g, 3.5 mmol), K_2CO_3 (1.0 g, 7.0 mmol), KI (0.12 g, 0.7 mmol), and compound **2** (2.0 g, 4.2 mmol) were dissolved in 50 mL of acetonitrile under nitrogen atmosphere. The mixture was heated to 80 °C and stirred at that temperature for 24 h. Excess potassium carbonate was filtered off. After solvent was evaporated, the solid was dissolved in ethyl acetate. The ethyl acetate solution was extracted with 5% hydrochloric acid, washed with water, saturated NaCl aqueous solution and dried over anhydrous $MgSO_4$. After solvent was removed, the crude product was purified by column chromatography (silica gel, hexane as eluent) to yield 1.65 g (91%) of white crystals; mp 52–53 °C. MS (EI, *m/z*): 516 (M^+). ^{1}H NMR ($CDCl_3$, δ ppm): 1.40–1.49 (m, 8H, $-OCH_2CH_2-(CH_2)_4-$), 1.73–1.88 (m, 4H, $-OCH_2CH_2-(CH_2)_4-CH_2-$), 3.77 (s, 3H, $-OCH_3$), 3.84 (s, 3H, $-OCH_3$), 3.87–3.97 (m, 4H, $-OCH_2-(CH_2)_6-CH_2O-$), 6.83 (s, 4H, aromatic-H), 7.26 (s, 2H, aromatic-H). ^{13}C NMR ($CDCl_3$, δ ppm): 25.6, 28.8, 28.9, 55.6, 55.8, 67.2, 68.1, 114.5, 115.2, 115.3, 116.1, 153.7, 154.1, 154.7, 157.0.

2.3.5. 1,4-Bis(4′-butylbiphenyl)-2-methoxy-5-[8-(4-methoxyphenoxy)octan-1-yloxy]benzene (*5*)

Compounds **3** (0.31 g, 0.6 mmol) and **4** (0.5 g, 1.5 mmol), K_2CO_3 (0.55 g), Aliquat 336 (0.1 g), and $Pd(PPh_3)_4$ (0.01 g, 0.01 mmol) were dissolved in a mixed solvent of toluene (20 mL) and degassed water (4 mL). The reaction mixture was refluxed with vigorous stirring for 48 h under argon atmosphere. Ethyl acetate (50 mL) was added into the mixture. The obtained solution was washed with brine and dried over magnesium sulfate. After evaporating the solvent, the crude product was purified by silica gel column chromatography using ethyl acetate/hexane (1:10 by volume) as eluent to yield 0.30 g (65%) of yellow crystals; mp 92–93 °C. MS (EI, *m/z*): 775 (M^+). ^{1}H NMR ($CDCl_3$, δ ppm): 0.96 (t, $J = 7.5$ Hz, 6H, $-C_3H_6-CH_3$), 1.31–1.44 (m, 12H, $-OCH_2CH_2-(CH_2)_4-$ and two $-CH_2-CH_3$), 1.60–1.71 (m, 8H, $-OCH_2CH_2-(CH_2)_4-CH_2-$ and two $-CH_2-CH_2-CH_3$), 2.64–2.69 (t, $J = 7.5$ Hz, 4H, $-CH_2-C_3H_7$), 3.76 (s, 3H, $-OCH_3$), 3.84 (s, 3H, $-OCH_3$), 3.94–3.98 (m, 4H, $-OCH_2-(CH_2)_6-CH_2O-$), 6.80 (s, 4H, aromatic-H), 7.05 (s, 2H, aromatic-H), 7.26–7.29 (m, 4H, aromatic-H), 7.57–7.59 (m, 4H, aromatic-H), 7.67–7.72 (m, 8H, aromatic-H). ^{13}C NMR ($CDCl_3$, δ ppm): 13.5, 22.3, 25.6, 28.9, 33.9, 35.4, 55.6, 55.8, 68.1, 68.3, 114.5, 115.3, 116.1, 120.0, 127.6, 128.7, 129.4, 134.4, 136.5, 139.5, 146.4, 152.3, 154.8, 157.1.

2.3.6. 1,4-Bis(4′-butylbiphenyl)-2-methoxy-5-[8-(2,5-dibromomethyl-4-methoxyphenoxy)octan-1-yloxy]benzene (*M1*)

Compound **5** (0.5 g, 0.6 mmol), paraformaldehyde (0.1 g, 3.3 mol), and 30% HBr in acetic acid (2 mL) were dissolved in 5 mL of acetic acid. The mixture was heated to 70 °C and kept at that temperature with stirring for 16 h. After cooling to room temperature, the reaction mixture was diluted with chloroform followed by extraction with water and 5% $NaHCO_3$ aqueous solution. The chloroform solution was dried over $MgSO_4$ followed by the removal of the chloroform under reduced pressure. The crude product was recrystallized from hexane to yield 0.33 g (54%) of **M6**; mp 97–98 °C. Element Anal.: calculated 69.93% C, 6.66% H; found 70.36% C, 6.53% H. ^{1}H NMR ($CDCl_3$, δ ppm): 0.96 (t, $J = 7.5$ Hz, 6H, two $-C_3H_6-CH_3$), 1.31–1.44 (m, 12H, $-OCH_2CH_2-(CH_2)_4-$ and two $-CH_2-CH_3$), 1.58–1.71 (m, 8H, $-OCH_2CH_2-(CH_2)_4-CH_2CH_2O-$ and two $-CH_2-CH_2-C_2H_5$), 2.67 (t, $J = 7.5$ Hz, 4H, two $-CH_2-C_3H_7$), 3.75 (s, 3H, $-OCH_3$), 3.85 (s, 3H, $-OCH_3$), 3.88–3.98 (m, 4H, $-OCH_2-(CH_2)_6-CH_2O-$), 4.50 (s, 4H, two $-CH_2Br$), 6.80 (s, 2H, aromatic-H), 7.05 (s, 2H, aromatic-H), 7.26–7.29 (m, 4H, aromatic-H), 7.57–7.59 (m, 4H, aromatic-H), 7.67 (m, 8H, aromatic-H). ^{13}C NMR ($CDCl_3$, δ ppm): 13.8, 22.4, 25.6, 28.6, 28.9, 33.9, 35.5, 55.6, 55.9, 68.2, 115.3, 117.5, 120.0, 125.8, 127.6, 128.7, 129.3, 134.3, 136.5, 139.6, 146.4, 152.3, 153.1, 153.8.

2.3.7. 1,4-Bis(4′-butylbiphenyl)-2-methoxy-5-[8-(2,5-dibromo-4-methoxyphenoxy)octan-1-yloxy]-benzene (*M2*)

Bromine (0.14 mL, 2.7 mmol) was added dropwise to a solution of compound **5** (0.7 g, 0.9 mmol) in chloroform (20 mL). The solution was stirred at room temperature for 12 h, and the excess bromine was quenched with sodium thiosulphate aqueous solution. The organic layers were combined, washed until neutral, and then dried over magnesium sulfate. The organic solvent was evaporated and obtained 0.73 g (87%) of a yellow powder; mp 103–104 °C. Element Anal.: calculated 69.53% C, 6.44% H; found 69.87% C, 6.26% H. ^{1}H NMR ($CDCl_3$, δ ppm): 0.96 (t, $J = 7.5$ Hz, 6H, two

$-C_3H_6-CH_3$), 1.31–1.44 (m, 12H, $-OCH_2CH_2-(CH_2)_4-$ and two $-CH_2-CH_3$), 1.58–1.71 (m, 8H, $-OCH_2CH_2-(CH_2)_4-CH_2CH_2O-$ and two $-CH_2-CH_2-C_2H_5$), 2.65–2.70 (t, $J = 7.5$ Hz, 4H, two $-CH_2-C_3H_7$), 3.76 (s, 3H, $-OCH_3$), 3.85 (s, 3H, $-OCH_3$), 3.88–3.98 (m, 4H, $-OCH_2-(CH_2)_6-CH_2O-$), 6.80 (s, 2H, aromatic-H), 7.05 (s, 2H, aromatic-H), 7.26–7.29 (m, 4H, aromatic-H), 7.57–7.59 (m, 4H, aromatic-H), 7.67–7.73 (m, 8H, aromatic-H). ^{13}C NMR ($CDCl_3$, δ ppm): 13.3, 22.1, 25.2, 28.8, 33.7, 35.6, 55.8, 55.5, 68.2, 68.6, 115.3, 120.2, 127.4, 128.5, 129.5, 134.6, 136.3, 139.4, 146.4, 152.2, 154.7, 157.4.

2.3.8. Model compound (*LC1*)

Compound **4** (0.5 g, 1.5 mmol), 1,4-dibromo-2,5-dimethoxybenzene (0.18 g, 0.6 mmol), K_2CO_3 (0.55 g), Aliquat 336 (0.1 g) and $Pd(PPh_3)_4$ (0.01 g, 0.01 mmol) were dissolved in a mixed solvent of toluene (20 mL) and degassed water (4 mL). The reaction mixture was refluxed with vigorous stirring for 48 h under argon atmosphere. Ethyl acetate (50 mL) was added. The obtained solution was washed with brine and dried over magnesium sulfate. After solvent was removed by rotary evaporation, the crude product was purified by silica gel column chromatography using ethyl acetate/hexane (1:10 by volume) as eluent to yield 0.24 g (72%) of white crystals; mp 148–149 °C. MS (EI, *m/z*): 554 (M^+). Element Anal.: calculated 86.52% C, 7.57% H; found 86.34% C, 7.46% H. ^{1}H NMR ($CDCl_3$, δ ppm): 0.96 (t, $J = 7.5$ Hz, 6H, two $-C_3H_6-CH_3$), 1.36–1.45 (m, 4H, two $-CH_2-CH_3$), 1.61–1.68 (m, 4H, two $-CH_2-CH_2-C_2H_5$), 2.67 (t, $J = 7.5$ Hz, 4H, two $-CH_2-C_3H_7$), 3.84 (s, 6H, $-OCH_3$), 7.05 (s, 2H, aromatic-H), 7.26–7.29 (m, 4H, aromatic-H), 7.56–7.59 (m, 4H, aromatic-H), 7.70 (s, 8H, aromatic-H). ^{13}C NMR ($CDCl_3$, δ ppm): 13.6, 22.3, 33.8, 35.5, 55.8, 115.6, 120.1, 127.6, 129.8, 134.6, 136.5, 137.4, 146.3, 152.3.

2.4. Preparation of polymers *PPV1–PPV4*

Scheme 2 outlines the synthetic routes for polymers **PPV1–PPV4**. Polymers **PPV1–PPV4** were prepared by polymerization of different ratios of monomers **M1** and **M2** via Gilch route [27]. The synthesis of **PPV1** was given as an example. Monomer **M1** (0.2 g, 0.2 mmol) was dissolved in 5 mL of THF and flushed with N_2. A THF solution of potassium *tert*-butoxide (2 mL, 1.0 M) was then added slowly. After complete addition of the base, the reaction mixture was stirred for additional 16 h. The solution was poured into rapidly stirred methanol, and the obtained polymer was collected by suction filtration. The polymer was dissolved in THF, reprecipitated several times into methanol, collected, and dried under reduced pressure to give 0.06 g (32%) of **PPV1**.

Yield of **PPV1**: 32%. Element Anal.: calculated 83.99% C, 7.88% H; found 83.29% C, 7.81% H. ^{1}H NMR ($CDCl_3$, δ ppm): 0.95–1.02 (m, alkyl protons), 1.26–1.33 (m, alkyl protons), 1.60–1.74 (m, alkyl protons), 2.60–2.67 (m, $-Ph-CH_2-$), 3.75 (s, $-OCH_3$), 3.83 (s, $-OCH_3$), 3.92–3.98 (m, $-OCH_2-$), 6.80 (s, vinyl-H), 7.04 (s, aromatic-H), 7.24–7.28 (m, aromatic-H), 7.50–7.72 (m, aromatic-H). ^{13}C NMR ($CDCl_3$, δ ppm): 13.8, 24.4, 26.1, 29.5, 37.8, 55.8, 56.7, 68.9, 70.1, 114.9, 115.7, 117.0, 126.5, 126.9, 127.3, 128.9, 129.9, 130.9, 137.3, 138.5, 140.0, 141.8, 150.7, 151.2.

Yield of **PPV2**: 48%. Element Anal.: calculated 82.56% C, 8.29% H; found 81.73% C, 8.47% H. ^{1}H NMR ($CDCl_3$, δ ppm): 0.94–1.00 (m, alkyl protons), 1.24–1.32 (m, alkyl protons), 1.66–1.70 (m, alkyl protons), 2.59–2.62 (m, $-Ph-CH_2-$), 3.74 (s, $-OCH_3$), 3.82 (s, $-OCH_3$), 3.94–3.99 (m, $-OCH_2-$), 6.70 (s, vinyl-H), 6.79 (s, vinyl-H), 7.04 (s, aromatic-H), 7.24–7.27 (m, aromatic-H), 7.54–7.65 (m, aromatic-H). ^{13}C NMR ($CDCl_3$, δ ppm): 13.6, 24.2, 26.2, 29.6, 37.5, 55.7, 56.6, 68.8, 70.1, 114.8, 115.6, 117.1, 126.3,

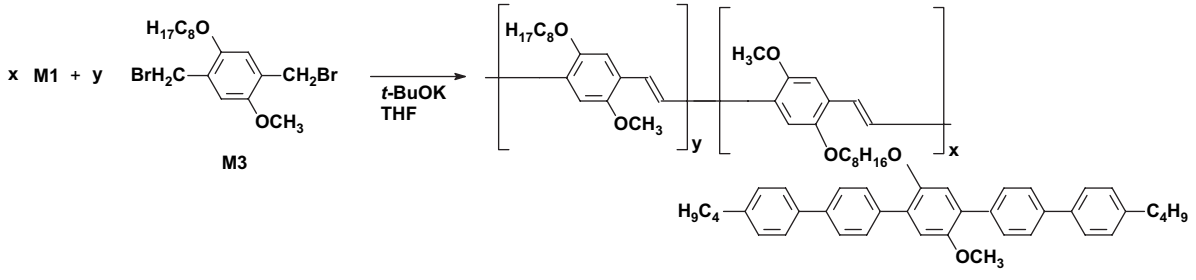

Polymer	x (M1%)	y (M3%)
PPV1	100	0
PPV2	50	50
PPV3	25	75
PPV4	10	90

Scheme 2. Synthesis of copolymers **PPV1–PPV4**.

126.8, 127.3, 128.8, 129.9, 130.8, 137.1, 138.4, 140.1, 141.9, 150.7, 151.3.

Yield of **PPV3**: 51%. Element Anal.: calculated 81.06% C, 8.71% H; found 79.81% C, 7.93% H. ^{1}H NMR ($CDCl_3$, δ ppm): 0.94–1.01 (m, alkyl protons), 1.23–1.31 (m, alkyl protons), 1.68–1.73 (m, alkyl protons), 2.57–2.61 (m, −Ph−CH_2−), 3.76 (s, −OCH_3), 3.82 (s, −OCH_3), 3.91–3.98 (m, −OCH_2−), 6.72 (s, vinyl-H), 6.81 (s, vinyl-H), 7.02 (s, aromatic-H), 7.24–7.28 (m, aromatic-H), 7.53–7.64 (m, aromatic-H). ^{13}C NMR ($CDCl_3$, δ ppm): 13.7, 24.4, 26.5, 29.5, 37.4, 55.9, 56.4, 68.7, 70.2, 114.5, 115.7, 117.2, 126.3, 126.5, 127.3, 128.9, 129.7, 130.8, 137.2, 138.3, 140.1, 141.7, 150.6, 151.6.

Yield of **PPV4**: 57%. Element Anal.: calculated 79.55% C, 9.10% H; found 77.96% C, 8.44% H. ^{1}H NMR ($CDCl_3$, δ ppm): 0.92–0.98 (m, alkyl protons), 1.25–1.33 (m, alkyl protons), 1.66–1.72 (m, alkyl protons), 2.58–2.64 (m, −Ph−CH_2−), 3.76 (s, −OCH_3), 3.81 (s, −OCH_3), 3.92–3.98 (m, −OCH_2−), 6.71 (s, vinyl-H), 6.79 (s, vinyl-H), 7.05 (s, aromatic-H), 7.23–7.27 (m, aromatic-H), 7.54–7.66 (m, aromatic-H). ^{13}C NMR ($CDCl_3$, δ ppm): 13.7, 24.4, 26.4, 29.7, 37.6, 55.8, 56.6, 68.7, 70.3, 114.5, 115.2, 117.3, 126.1, 126.6, 127.4, 128.8, 129.7, 130.6, 137.3, 138.5, 140.2, 141.8, 150.8, 151.5.

2.5. Preparation of polymers *PF1–PF5*

Scheme 3 outlines the synthetic routes for polymers **PF1–PF5**. Polymers **PF1–PF5** were prepared via Suzuki coupling of monomer **M4** with **M2** and/or **M5–M7** [28–30]. The synthesis of **PF1** was given as an example. Monomers **M2** (0.1 g, 0.11 mmol), **M4** (0.17 g, 0.27 mmol), **M5** (0.09 g, 0.16 mmol), K_2CO_3 (0.55 g), Aliquat 336 (0.1 g) and $Pd(PPh_3)_4$ (0.01 g, 0.01 mmol) were dissolved in a mixed solvent of toluene (10 mL) and degassed water (2 mL). The reaction mixture was refluxed with vigorous stirring for 72 h under argon atmosphere. At the end of polymerization, the end capping reagents (1-bromo-4-(*tert*-butyl) benzene and 1-(*tert*-butyl)-4-(4,4,5,5-tetramethyl-1,3,2-dioxaborolan-2-yl) benzene) were added and the resulting solution was stirred for 24 h. The solution was poured into methanol to precipitate the polymer. A powdered solid was obtained by filtration. The polymer was dissolved in THF and reprecipitated several times into methanol and then dried under vacuum to yield 0.16 g (45%) of **PF1**.

Yield of **PF1**: 45%. Element Anal.: calculated 88.09% C, 10.25% H; found 87.34% C, 9.46% H. ^{1}H NMR ($CDCl_3$, δ ppm): 0.83–0.90 (m, alkyl protons), 0.96–1.25 (m, alkyl protons), 1.55–1.84 (m, alkyl protons), 2.59–2.67 (m, −Ph−CH_2−), 3.74 (s, −OCH_3), 3.84 (s, −OCH_3), 3.87–3.97 (m, −OCH_2−), 6.67–6.78 (m, aromatic-H), 7.04–7.08 (m, aromatic-H), 7.24–8.01 (m, aromatic-H). ^{13}C NMR ($CDCl_3$, δ ppm): 13.9, 22.5, 23.9, 29.7, 31.5, 32.3, 34.7, 37.5, 55.5, 66.4, 114.5, 120.1, 121.8, 126.6, 129.8, 140.8, 146.5, 152.1.

Yield of **PF2**: 46%. Element Anal.: calculated 87.27% C, 9.84% H; found 86.14% C, 8.73% H. ^{1}H NMR ($CDCl_3$, δ ppm): 0.82–0.88 (m, alkyl protons), 0.94–1.24 (m, alkyl protons), 1.54–1.82 (m, alkyl protons), 2.58–2.66 (m, −ph−CH_2−), 3.74 (s, −OCH_3), 3.83 (s, −OCH_3), 3.86–3.97 (m, −OCH_2−), 6.68–6.79 (m, aromatic-H), 7.03–7.08 (m, aromatic-H), 7.22–8.02 (m, aromatic-H). ^{13}C NMR ($CDCl_3$, δ ppm): 13.8, 22.6, 23.9, 29.6, 31.4, 32.4, 34.6, 37.3, 55.7, 66.1, 114.3, 120.2, 121.7, 126.5, 129.7, 140.6, 146.5, 152.0.

Yield of **PF3**: 32%. Element Anal.: calculated 85.98% C, 9.19% H; found 84.47% C, 8.09% H. ^{1}H NMR ($CDCl_3$, δ ppm): 0.82–0.87 (m, alkyl protons), 0.94–1.23 (m, alkyl protons), 1.53–1.81 (m, alkyl protons), 2.56–2.64 (m, −ph−CH_2−), 3.73 (s, −OCH_3), 3.83 (s, −OCH_3), 3.87–3.98 (m, −OCH_2−), 6.67–6.79 (m, aromatic-H), 7.02–7.08 (m, aromatic-H), 7.23–8.02 (m, aromatic-H). ^{13}C NMR ($CDCl_3$, δ ppm): 13.9, 22.8, 23.7, 29.4, 31.2, 32.7, 34.5, 37.1, 55.8, 66.4, 114.2, 120.1, 121.6, 126.6, 129.8, 140.5, 146.4, 152.1.

Yield of **PF4**: 42%. Element Anal.: calculated 85.39% C, 9.39% H, 0.98% N; found 84.47% C, 8.98% H, 0.82% N. ^{1}H NMR ($CDCl_3$, δ ppm): 0.80–0.87 (m, alkyl protons), 1.23–1.26 (m, alkyl protons), 1.57–1.85 (m, alkyl protons), 2.55–2.64 (m, −ph−CH_2−), 3.74 (s, −OCH_3), 3.83 (s, −OCH_3), 3.77–3.87 (m, −OCH_2−), 6.67–6.78 (m, aromatic-H), 7.04–7.08 (m, aromatic-H), 7.24–8.01 (m, aromatic-H). ^{13}C NMR ($CDCl_3$, δ ppm): 13.9, 22.5, 24.0, 29.7, 31.5, 32.3, 34.7, 37.5, 52.8, 66.4, 114.2, 120.0, 121.8, 126.3, 129.9, 140.8, 146.7, 151.9.

Yield of **PF5**: 39%. Element Anal.: calculated 84.88% C, 9.29% H, 0.96% N; found 84.82% C, 8.81% H, 1.05% N. ^{1}H NMR ($CDCl_3$, δ ppm): 0.80–0.88 (m, alkyl protons), 1.22–1.26 (m, alkyl protons), 1.56–1.84 (m, alkyl protons), 2.54–2.66 (m, −ph−CH_2−), 3.73 (s, −OCH_3), 3.83 (s, −OCH_3), 3.78–3.89 (m, −OCH_2−), 6.66–6.78 (m, aromatic-H), 7.03–7.08 (m, aromatic-H), 7.23–8.02 (m, aromatic-H). ^{13}C NMR ($CDCl_3$, δ ppm): 13.8, 22.4, 24.1, 29.6, 31.7, 32.5, 34.7, 37.4, 52.8, 66.4, 114.3, 120.1, 121.7, 126.2, 129.8, 132.5, 140.5, 146.4, 152.2.

2.6. Fabrication of polarized EL devices

Polarized EL devices were fabricated on indium tin oxide (ITO)-coated glass substrates cleaned sequentially in ultrasonic baths of detergent, de-ionized water, 2-propanol, de-ionized water, and acetone. UV–ozone treatment was taken for 3 min as the final cleaning step to improve the contact angle just before film forming. Onto the ITO glass a layer of PEDOT–PSS film was spin-cast from its aqueous dispersion. After baking at 120 °C for 1 h, the PEDOT was rubbed by a rubbing machine and used as an alignment layer. The polymers were dissolved in toluene and the obtained solutions were spin-coated on the top of rubbed PEDOT layer. After annealing for 1 h, 35 nm calcium and 100 nm aluminum cathodes were deposited onto the top of an aligned emitting film by thermal evaporation through a shadow mask.

3. Results and discussion

3.1. Synthesis and thermal properties

Table 1 lists the polymerization results and phase transition temperatures of polymers **PPV1–PPV4** and **PF1–PF5**. The

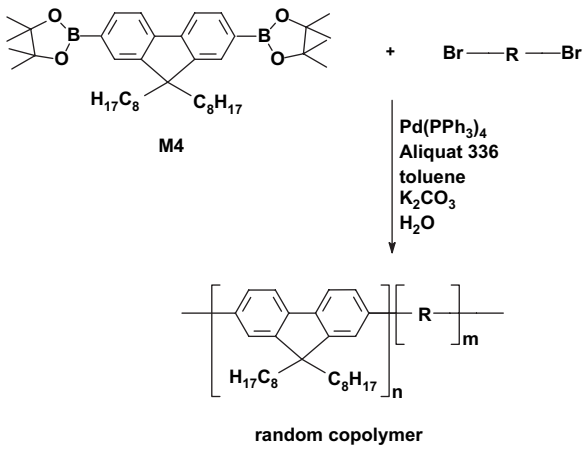

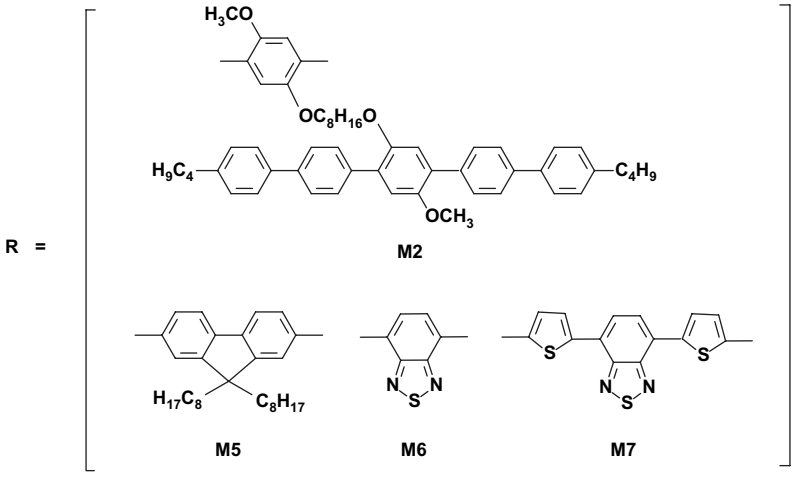

Polymer	**M2**(%)	**M4**(%)	**M5**(%)	**M6**(%)	**M7**(%)
PF1	10	50	40	-	-
PF2	20	50	30	-	-
PF3	40	50	10	-	-
PF4	20	50	15	15	-
PF5	20	50	15	10	5

Scheme 3. Synthesis of polymers **PF1**–**PF5**.

Table 1
Polymerization results and phase transition temperatures of copolymers

Copolymer	Yield (%)	$\overline{M}_n$	$\overline{M}_w$	PDI	Phase transition temperatures[a] (°C)							T_d[b] (°C)
PPV1	32	8600	13 100	1.52	G	48	K	112	N	327	I	340
PPV2	48	35 800	63 200	1.73	G	54	K	116	N	322	I	357
PPV3	51	39 300	70 900	1.81	G	61	K	124	N	306	I	372
PPV4	57	85 600	185 300	1.85	G	65	K	128	N	308	I	388
PF1	45	8100	12 800	1.58		G	75	N	296	I		374
PF2	46	8300	12 100	1.46		G	76	N	302	I		368
PF3	35	6500	9300	1.43		G	73	N	258	I		340
PF4	42	7400	9800	1.32		G	80	N	297	I		416
PF5	39	6200	9600	1.55		G	81	N	300	I		422

[a] The temperatures were observed by DSC. G: glassy; K: crystalline; N: nematic; I: isotropic.
[b] The temperatures were observed by TGA.

number average molecular weights of **PPV1**–**PPV4** are in the range from 8.6×10^3 to 8.56×10^4. The bulky mesogenic side group affects dramatically the degree of polymerization. Homopolymer **PPV1**, with 100% of **M1** units, shows a lowest molecular weight while **PPV4**, with the lowest content (10%) of **M1** units, achieves the highest molecular weight. Fig. 2A presents the DSC thermograms of **LC1**. The heating scan shows a crystal to nematic phase transition at 161 °C, and a nematic to isotropic phase transition (T_{N-I}) at 204 °C. The cooling scan shows an isotropic to nematic phase transition at 196 °C, and a nematic to crystal phase transition at 138 °C. Fig. 2B depicts a DSC thermogram of **PPV1** which shows a glass transition temperature at 48 °C, a crystal to nematic phase transition at 112 °C, and a nematic to isotropic phase transition at 327 °C. Fig. 3A and B shows the typical nematic textures exhibited by **PPV1** and **LC1**. As the sequence from **PPV1** to **PPV4**, the bulky monomer **M1** content decreases while the **M2** content increases. All four polymers exhibit nematic liquid crystalline behavior. According to the literature [31], similar PPVs without mesogenic side group show only a glass transition around 50 °C. However, the synthesized **PPV1**–**PPV4** shows very complex thermal behavior,

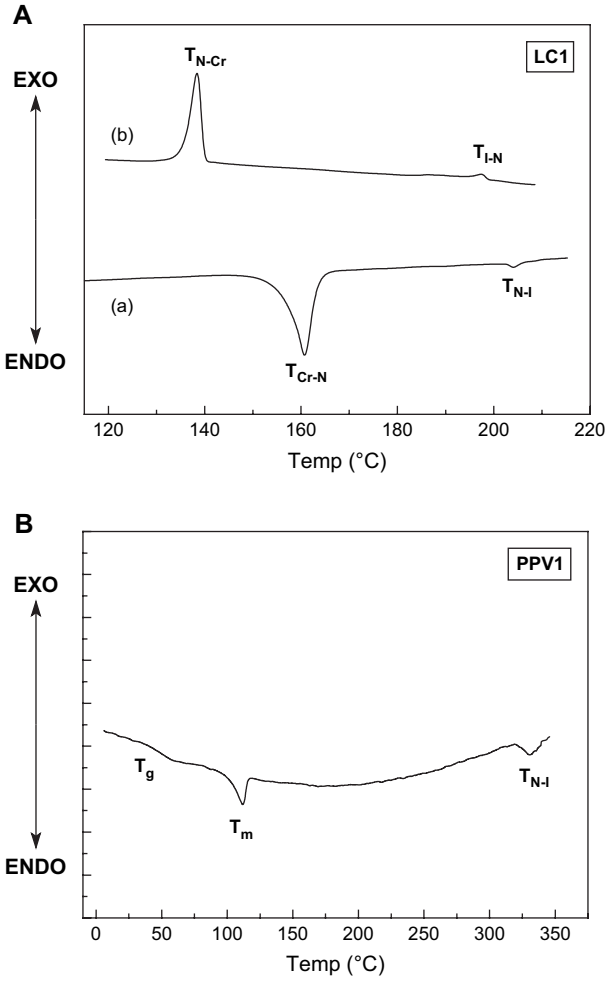

Fig. 2. (A) DSC thermogram of model compound **LC1** (a) heating scan and (b) cooling scan; (B) DSC thermogram of polymer **PPV1**.

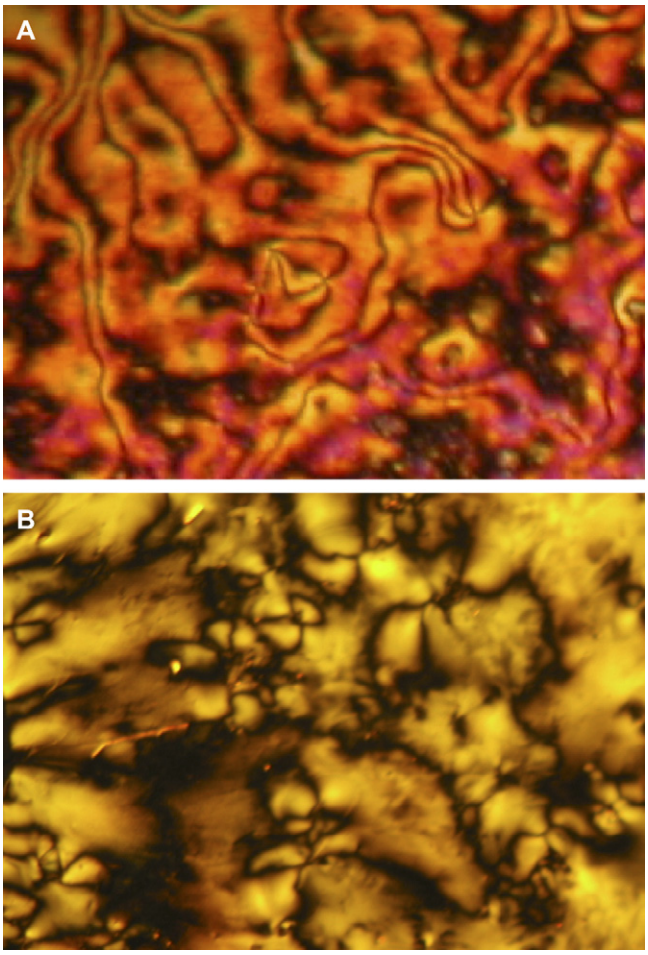

Fig. 3. (A) Polarized optical micrograph of **LC1** at 170 °C. (B) Polarized optical micrograph of polymer **PPV1** at 150 °C.

which contain T_g, T_m and T_{N-I}. These polymers eventually show microphase separation behavior, which is very common for side-chain liquid crystal polymers. It is well-documented in the literatures [32] that a microphase separated side-chain polymers should contain microdomains exclusively of polymer backbone and microdomains exclusively of mesogenic side groups. The glass transition is due to the segmental motion of the polymer backbone microdomains. Both T_m and T_{N-I} are attributed to the thermal behavior of mesogenic side groups' microdomains. The mesogenic side groups show very similar thermal behavior with the model compound, which show both T_m and T_{N-I}. All four polymers are thermally stable and their thermal degradation temperatures are higher than 340 °C.

The number average molecular weights ($\overline{M}_n$) of **PF1**–**PF5** are in the range of 6.2×10^3–8.3×10^3. The reason could be due to the bulky monomer unit **M2** which affects the degree of polymerization. Table 1 also summarizes the thermal transition of **PF1**–**PF5**. All five polymers present nematic liquid crystalline behavior. Their glass transition temperatures are around 75 °C and isotropization temperatures are in the range from 258 to 302 °C. According to literatures [12–15], polyfluorenes without the mesogenic side groups exhibit also

nematic liquid crystalline behavior. As consequence, both main-chain and side-chain segments of **PF1–PF5** have contribution to the formation of a nematic phase. However, due to the complicated combinations of different monomer units, it has difficulty to find the order tendency for both transitions.

3.2. Polarized optical properties

Aligned samples were prepared by annealing the polymers on a glass plate whose surface was pre-coated with PEDOT and rubbed by a mechanical rubbing technique. This peculiar procedure permits the polymer film to be aligned in the rubbing direction. To check the anisotropy of the aligned polymer films of **PPV1–PPV4** and **PF1–PF5**, polarized UV–vis absorption and PL emission spectra of these films were measured and the results are summarized in Table 2. Fig. 4A and B shows polarized UV absorption spectra and PL emission spectra of an aligned **PPV1** film which exhibited a pronounced optical anisotropy as expressed by the polarized ratios (defined as the ratio of parallel to perpendicular UV absorption peak intensity) of 5.2 at 350 nm and 5.1 at 517 nm. The absorbance and emission in the parallel direction were obviously higher than those in the perpendicular direction, which indicated that annealing these polymers at their liquid crystalline phase could thus induce alignment predominantly along the rubbing direction. The absorption at 350 nm was corresponded to the expected π–π* transition from the penta(*p*-phenylene) liquid crystalline side group, where as the absorption at 517 nm was corresponded to the expected π–π* transition from the PPV backbone. Fig. 4B shows two PL emission bands for polymer **PPV1**. The yellow emission band (572 nm) is due to the emission from the PPV main chains and blue emission band (406 nm) is due to the emission from penta(*p*-phenylene) liquid crystalline side groups. The polarized ratios show 4.7 at 406 nm and 4.5 at 572 nm for PL emissions, which is superior to the side-chain liquid crystalline PPVs reported previously [8,21]. Fig. 5 shows polarized UV and PL spectra of an aligned **PF1** film. An UV absorption maximum was observed at 319 nm, which revealed π–π* transition of the **PF1** backbone (all absorption wavelengths are listed in Table 2). Since the feed ratio of mesogen-containing monomer **M2** was only 10%, the absorption intensity of lateral mesogens was relatively low as compared with **PF1** main chain. This is different from Fig. 4A, where a strong absorption band was found at 350 nm, referring to lateral mesogens. According to the data shown in Table 2, the UV–vis and PL polarized ratios of **PF1–PF5** are higher than 11.2. This means that the aligned PF films showed more pronounced optical anisotropy than

Table 2
The polarized UV–vis absorption, polarized PL emission and polarized ratio of copolymers

Copolymer	Polarized UV_{max}–vis absorption (nm)	Polarized PL_{max} emission (nm)	Polarized ratio	
			UV–vis ($UV_{\parallel}/UV_{\perp}$)	PL ($PL_{\parallel}/PL_{\perp}$)
PPV1	350(517)	406(572)	5.2(5.1)	4.7(4.5)
PPV2	350(516)	406(574)	3.8(3.5)	3.3(3.1)
PPV3	352(517)	408(574)	3.6(3.5)	3.3(2.9)
PPV4	352(518)	408(580)	3.2(3.1)	3.1(2.9)
PF1	319	416	12.6	11.2
PF2	320	419	13.2	12.7
PF3	319	416	13.1	12.6
PF4	435	536	15.5	14.2
PF5	516	648	13.5	13.3

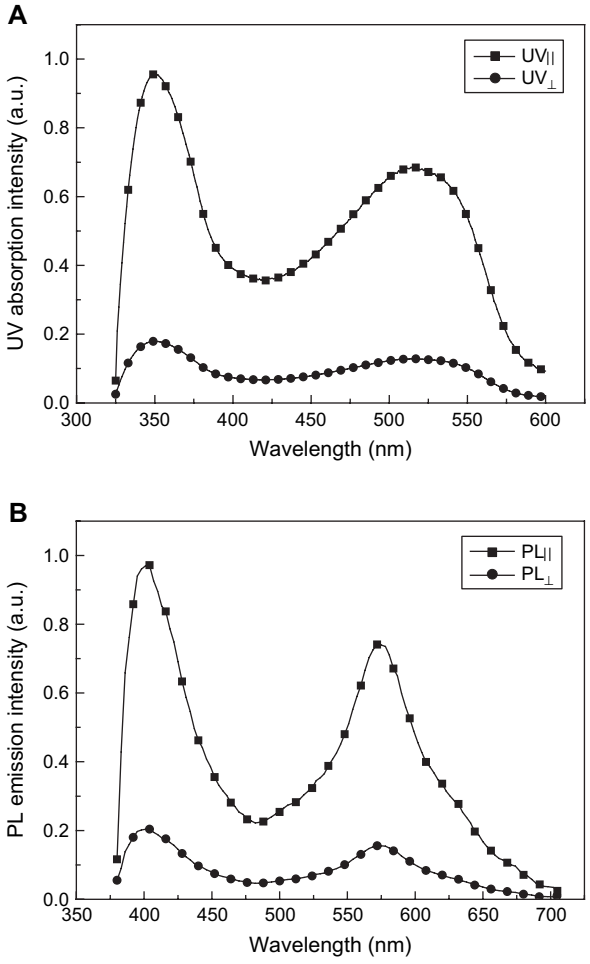

Fig. 4. (A) Polarized UV–vis absorption spectra of **PPV1**. (B) Polarized PL emission spectra of **PPV1**.

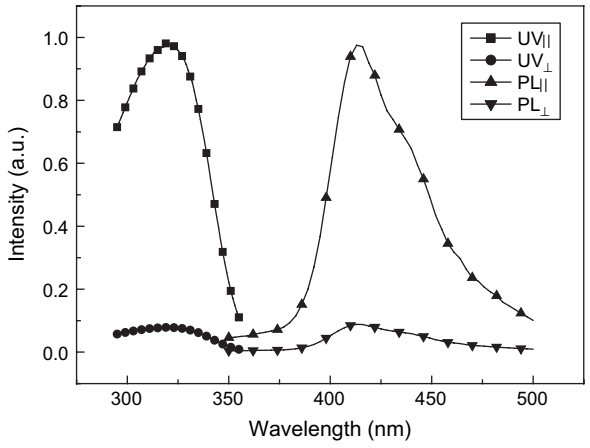

Fig. 5. Polarized UV–vis absorption spectra and polarized PL emission spectra of **PF1**.

the aligned PPV films. The results are reasonable because the PF backbones are involving in the formation of a nematic phase while PPV main chains are not. **PF1–PF3** emit ultraviolet to blue light at around 416 nm which is associated with both polyfluorene backbones and penta(*p*-phenylene) side groups **PF4** and **PF5** revealed two emission peaks at 416 nm and 536 nm. The former is associated with the penta(*p*-phenylene) side groups while the latter is attributed to benzothiadiazole moiety in the main chains.

3.3. Polarized EL property

Double-layers PLED devices with the configuration of ITO/rubbed PEDOT–PSS/emitting polymer/Ca/Al were fabricated for the measurements of polarized EL spectra. The results are summarized in Table 3. Basically **PPV1–PPV4** reveal very similar EL behavior. Fig. 6A and B reports the representative polarized EL spectra and device properties of **PPV4** which emits yellow light at 588 nm. Its maximum luminance and polarized ratio are 1337 cd/m^2 and 2.6, respectively. Again, the low polarized ratios of **PPV1–PPV4** devices are basically due to the poor alignment of PPV backbones. Since penta(*p*-phenylene) side groups emit ultraviolet to blue light, the EL emission at 588 nm should be attributed to PPV main chains only.

As can be seen from Table 3, **PF1–PF3** emit ultraviolet to blue light at 428 nm while **PF4** and **PF5** emit, respectively, a green light at 540 nm and an orange-red light at 650 nm. A complete energy transfer from penta(*p*-phenylene) side groups to PF main chains was observed. Fig. 7 depicts the UV–vis and PL spectra of model compound **LC1**. The PL emission of **LC1** is overlapped with the UV absorption peak of **PF4**. This provides a route for energy transfer [18,19,33]. Instead, PPVs showed a UV absorption around 516–518 nm, which is not overlapped with the emission of **LC1**. Hence, no energy transfer was found in this case. The polarized ratios of **PF1–PF5** are higher than 9.5. The highest luminance and polarized ratio are 1855 cd/m^2 and 12.4, respectively, achieved by **PF4**.

To generate a polarized white light, PLED device is the main goal of this study. We use **PF2** as a host polymer and **PF4** and **PF5** as guest polymers. Simply blending small amounts of **PF4** and **PF5** into **PF2** can fabricate a white light

Table 3
EL properties and polarized ratio using copolymers as active layers

Copolymer	EL (nm)	$V_{turn\ on}$ (V)	Luminance (cd/m^2)	Yield (cd/A)	Polarized ratio
PPV1	584	5	163	0.07	3.6
PPV2	584	5	401	0.16	3.3
PPV3	588	5	534	0.17	3.2
PPV4	588	4	1337	0.33	2.6
PF1	428	6	469	0.06	12.6
PF2	428	6	525	0.07	11.9
PF3	432	7	403	0.06	9.5
PF4	540	5	1855	0.57	12.4
PF5	652	6	1052	0.17	10.7

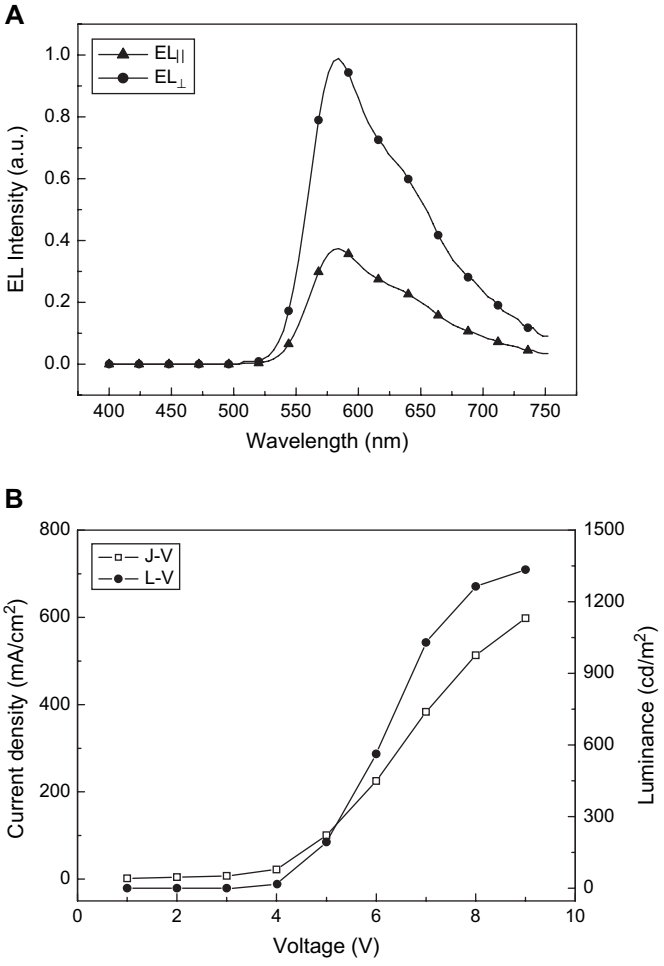

Fig. 6. (A) Polarized EL spectra of **PPV4** in the ITO/aligned PEDOT/**PPV4**/Ca/Al device; (B) J–V(□) and L–V(●) curves of **PPV4** in the ITO/aligned PEDOT/**PPV4**/Ca/Al device.

device. Fig. 8A shows the polarized white light EL spectra of a PLED device generated by blending 0.04 and 0.06 wt% of **PF4** and **PF5** with **PF2**. The maximum luminance and polarized ratio are 483 cd/m^2 and 11.6, respectively, with CIE coordinate (0.34,0.35) which is very close to pure white light. The

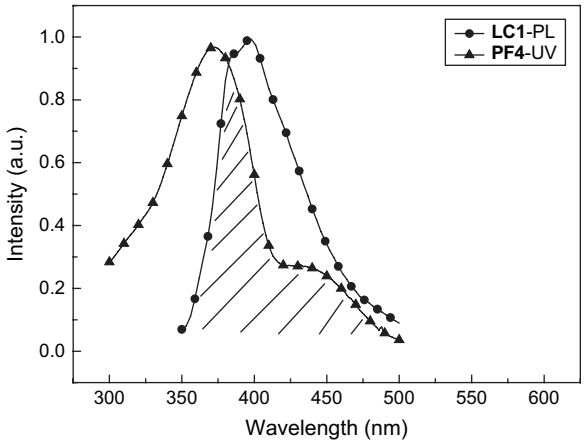

Fig. 7. Absorption and emission spectra of **PF4** and **LC1**.

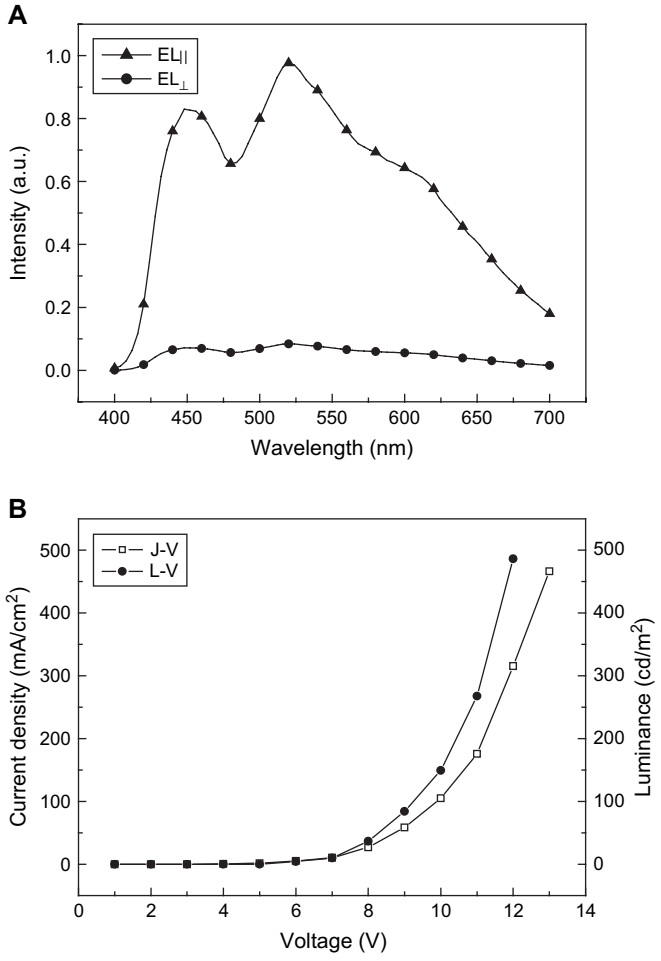

Fig. 8. (A) Polarized EL spectra of device A in ITO/aligned PEDOT/polymer **PF2** + **PF4** + **PF5**/Ca/Al device; (B) J–V (□) and L–V (●) curves of device A in ITO/aligned PEDOT/polymer **PF2** + **PF4** + **PF5**/Ca/Al device.

Table 4
Properties of polarized white emission devices

Device	**PF2**:**PF4**:**PF5** (wt%)	$V_{turn\ on}$ (V)	Luminance (max) (cd/m^2)	Polarized ratio ($EL_{\|}/EL_{\perp}$)	CIE 1931 (x,y)
A	100:0.04:0.06	6	483	11.6	(0.339,0.354)
B	100:0.06:0.06	6	916	11.8	(0.343,0.381)
C	100:0.08:0.08	6	2454	10.2	(0.352,0.397)

best result is achieved in device C (Table 4) with 0.08 wt% of **PF4** and **PF5**. Its maximum luminance and polarized ratio are 2454 cd/m^2 and 10.2, respectively. For practical application EL polarization ratios of 30–40 are required, but with the use of a clean-up polarizer, EL ratios of 10 or more are adequate [34]. At present polarized white light devices fabricated in this work showed highest brightness with moderate polarization ratio. With further improvement of luminance efficiencies of device, these EL devices are believed to be applicable to LCD backlights.

4. Conclusions

Two series of new PPV and PF derivatives containing lateral attached penta(*p*-phenylene) mesogens were synthesized and characterized. Both series of polymers revealed nematic liquid crystalline behavior and were suitable for the fabrication of polarized EL devices. The PPV derivatives emit a yellow light while PF derivatives emit RGB three primary lights depending on the composition of monomer units in the backbones. The PLED devices based on PF derivatives show much higher polarized ratios than those based on PPV derivatives because both PF main chains and penta(*p*-phenylene) side groups are involving in the formation of a nematic phase while PPV main chains are not. The synthesized PF derivatives were useful for the fabrication of polarized white PLED devices. Blending small amount of **PF4** and **PF5** with a host **PF2** achieved a white PLED device with highest luminance of 2454 cd/m^2, polarized ratio of 10.2 and CIE coordinate of (0.35,0.39) which had potential application in LCD backlight.

Acknowledgements

The authors are grateful to the National Science Council (NSC92-2216-E009-015) and Ministry of Education (MOE ATU program) of the Republic of China for financial support for this work.

References

[1] Burroughes JH, Bradley DDC, Brown AR, Marks RN, Mackay K, Friend RH, et al. Nature 1990;347:539.
[2] Peng Z, Bao Z, Galvin ME. Adv Mater 1998;10:680.
[3] Bliznyuk V, Ruhstaller B, Brock PJ, Scherf U, Carter SA. Adv Mater 1999;11:1257.
[4] Politis JK, Curtis MD. Chem Mater 2000;12:2798.
[5] Woodruff M. Synth Met 1996;80:257.
[6] Dyeklev P, Berggren M, Inganas O, Adersson MR, Wennerstorm O, Hjertberg T. Adv Mater 1995;7:43.
[7] Goto H, Akagi K. Macromolecules 2002;35:2545.
[8] Akagi K, Oguma J, Shibata S, Toyoshima R, Osaka I, Shirakawa H. Synth Met 1999;102:1287.
[9] Chen LX, Bao Z, Sapjeta BJ, Lovinger AJ, Crone B. Adv Mater 2000; 12:344.
[10] Jandke M, Strohriegl P, Gmeiner J, Brutting W, Schwoerer M. Adv Mater 1999;11:1518.
[11] Misaki M, Ueda Y, Nagamatsu S, Yoshida Y, Tanigaji N, Yase K. Macromolecules 2004;37:6926.
[12] Neher D. Macromol Rapid Commun 2001;22:1365.
[13] Miteva T, Meisel A, Knoll W, Nothofer HG, Scherf U, Mller DC, et al. Adv Mater 2001;13:565.
[14] Grell M, Knoll W, Lupo D, Meisel A, Mikeva T, Neher D, et al. Adv Mater 1999;11:671.
[15] Grell M, Bradley DDC, Woo EP, Inbasekaran M. Adv Mater 1997;9: 798.
[16] Sung HH, Lin HC. J Polym Sci A Polym Chem 2005;43:2700.
[17] Culligan SW, Geng Y, Chen SH, Klubek KP, Vaeth KM, Tang CW. Adv Mater 2003;15:1176.
[18] Chen ACA, Culligan SW, Geng Y, Chen SH, Klubek KP, Vaeth KM, et al. Adv Mater 2004;16:783.
[19] Chung SF, Wen TC, Chou WY, Guo TF. Jpn J Appl Phys 2006;45:L60.
[20] Yao YH, Kung LR, Hsu CS. Jpn J Appl Phys 2005;44:7648.
[21] Li AK, Yang SS, Jean WY, Hsu CS. Chem Mater 2000;12:2741.
[22] Zhou QF, Li HM, Feng XD. Macromolecules 1987;20:233.
[23] Pugh C, Schrock RR. Macromolecules 1992;25:6593.
[24] Gopalan P, Ober CK. Macromolecules 2001;34:5120.
[25] Gopalan P, Zhang Y, Li X, Wiesner U, Ober CK. Macromolecules 2003;36:3357.

[26] Cherodian AS, Highes NJ, Richardson RM, Lee MSK, Gray GW. Liq Cryst 1993;14:1667.
[27] Neef CJ, Ferraris JP. Macromolecules 2000;33:2311.
[28] Ranger M, Rondeau D, Leclerc M. Macromolecules 1997;30:7686.
[29] Herguth P, Jiang X, Liu MS, Jen AKY. Macromolecules 2002;35:6094.
[30] Hou Q, Zhou Q, Zhang Y, Yang W, Yang R, Cao Y. Macromolecules 2004;37:6299.
[31] Lutsen L, Adriaensens P, Becker H, Breemen AJV, Vanderzande D, Gelan J. Macromolecules 1999;32:6517.
[32] Percec V, Pugh C. Side chain liquid crystal polymers. In: McArdle CB, editor. New York: Chapman and Hall. p. 30 [chapter 3].
[33] Gong X, Moses D, Heeger AJ, Xiao SJ. Phys Chem B 2004;108:8601.
[34] Contoret AEA, Farrar SR, Jackson PO, Khan SM, May L, O'Neill M, et al. Adv Mater 2000;12:971.